10th ANKARA INTERNATIONAL AEROSPACE CONFERENCE **AIAC-2019-069**
18-20 September 2019 - METU, Ankara TURKEY

STATIC STRUCTURAL AND CFD ANALYSIS OF ROCKET NOZZLES MADE FROM MOLYBDENUM AND TITANIUM

Ömer Ali Günaltay[1]
Samsun University
Samsun, Turkey

Melahat Cihan[2]
Samsun University
Samsun, Turkey

ABSTRACT

In this paper we investigated the design and flow differences of two different nozzle geometries and their structural effects on two different materials. A conical shaped nozzle and an 80% bell shaped nozzle is designed for a certain operating condition. After designing the nozzles, CFD analysis has been done with ANSYS software, obtaining the Mach number, total pressure and temperature presentation inside the nozzle and investigating the flow behavior differences between the two nozzles. With the results of the CFD analyses, a static structural analysis has been done for Molybdenum and Titanium with ANSYS software and the flow effects on the structures were investigated.

[1] B.S. in Department of Aerospace Engineering, Email: omeraligunaltay@gmail.com
[2] Asst. Prof. in Department of Aerospace Engineering, Email: melahat.cihan@samsun.edu.tr

INTRODUCTION

In many cases, the main concern with flows that are subsonic is that they may be treated as incompressible. For rocket nozzles, flows are investigated which are supersonic, which are flows with a Mach number greater than 1.

Mach number is found by dividing the object speed by the local speed of sound. The Mach number determines the magnitude of many of the compressibility effects. It is called after Ernst Mach, a physicist who studied gas dynamics in the 19th century [Stark et al, 2007].

Rocket nozzles are mechanical devices without any rotating component inside, used to convert the thermal energy and pressure, which are being formed in the thrust chamber of the rocket engine, into kinetic energy. The pressure, temperature and velocity values should be available at particular sections to be able to design the geometry of the nozzle. The conical-shaped nozzle was used in early rocket applications because it is simple and easy to construct. It gets its name from the constant divergence angle of the wall. A smaller angle will increase the thrust because of the axial part of the exit velocity. However, it comes with the cost of a longer so heavier nozzle that is much more difficult to build. It is the opposite for large divergence angles but larger angles reduce the performance at low altitude because of the high outer pressure. Exhaust gas behavior can be seen in Fig. 1.

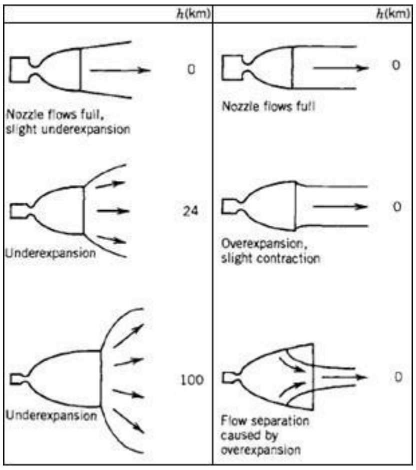

Figure 1 : Simplified sketches of exhaust gas behavior [Sutton et al, 2000]

The convergent-divergent nozzle is mostly used when the nozzle pressure is high. Performance engines in supersonic vehicles generally have a sort of convergent-divergent nozzle. The main purpose of the nozzle is to obtain a greater velocity of exhaust gas before discharge from the exit and to collect the flow, resulting in straightening the gas flow.

The Bell-shaped nozzle is the mostly used shaped rocket nozzle. With high angle expansion sections (20-50 degrees) after the nozzle throat followed by the bell like contour slope at the exit with a small divergence angle which is mostly less than 10 degrees. An ideal nozzle is one that leads all the gases from the thrust camber out the nozzle fully straight, which means that the moment of those gases would be axial. The Bell nozzle is designed to expand the gases with a large angle right after the throat. The diverging section is then curved back to create an almost straight flow of gas out of the nozzle exit. This large expansion creates expansion shock waves near the throat but the curving back of the diverging section causes compression shock waves, which cancels out the expansion shock waves by coincing, if correctly designed [Sutton, 2000 and Besnard, 2004].

Chapman at all, has reported the results of experimental and theoretical research conducted on flow separation in the 1950's to better recognize flow separation in supersonic nozzles and many activities are still being done today [Besnard et al, 2004].

Authors [Chapman et al, 1958, Stark, 2005 and Besnard, 2004] tried to enhance existing engineering criteria aiming for maximizing the nozzle expansion ratio without having a flow separation occur at sea level conditions. A compilation of those criteria has been gathered by Stark [Stark, 2005]. Stark, makes it obvious that the flow separation occurrence depends on several parameters like the wall actual conditions, the nozzle design, the operating conditions and fuel composition. Stark's study shows that the flow separation occurs at a static pressure value, which ranges from 0.25 to 0.4 times the ambient pressure.

Rao, developed a method for determining the nozzle contour for producing maximum thrust for a given expansion ratio and length [Rao, 1958]. This method turned out not only more efficient but also reducing the length of a 15-degree nozzle by 20-40% with the same area ratio. Sutton [Sutton et al, 2000], who worked with Rao, said that "bell shape or curved exit contour is used almost universally today for nozzles designed since about 1960 for large as well as small thrust chamber nozzles."

Östlund [Östlund et al, 1999] also projected some other design configurations in the 1990's, aiming to get rid of the flow separation and its drawbacks by investigating the bell nozzle. Other designs have also been projected like the dual-bell nozzles [Stark et al, 2007] and aerospike nozzles [Besnard et al, 2007].

This research will investigate and verify the advantages of the bell nozzle to the conical nozzle for a certain condition.

DESIGN OF CONICAL-SHAPED NOZZLE

The conical-shaped nozzle was used in early rocket applications because it is simple and easy to construct. It gets its name from the constant divergence angle of the wall. A smaller angle will increase the thrust because of the axial part of the exit velocity, V_e. However, it comes with the cost of a longer so heavier nozzle that is much more difficult to build. It is the opposite for large divergence angles but larger angles reduce the performance at low altitude because of the high outer pressure [Sutton et al, 2000].

Operating Conditions

Before starting calculations, some design parameters have to be set for the throat temperature and throat pressure. To be able to calculate those parameters a thrust chamber pressure and chamber temperature must be chosen. A temperature between 2000 and 3500 Kelvin is reasonable, also the chamber pressure can be thought between 0.5 and 50 MPa [Sutton et al, 2000]. Gasoline and Gaseous Oxygen is used for fuel as recommend for amateur rocketry in [9], which has a Specific Impulse of 240 sec. Thermodynamic properties were found using gas tables [Keenan et al, 1983]. Decisions made are shown in Table 1 taking in consider possible future tests.

Table 1: Design Parameters of Nozzle

Propellant	Thrust (F)	Specific Impulse (I_{sp})	Mass Flow ($\dot{m}$)	Molecular Weight (M)	Specific Heat Ratio (γ)	Chamber Temp. (T_c)	Chamber Pressure (P_c)
G-GOX	2000 N	240 sec	2.92 kg/s	24 g/mol	1.25	3000 K	2 MPa

Conical-shaped Nozzle Design Calculations

The equations used in this section are found in Ref. [Sutton et al, 2000] and Ref. [Peters, 1965]. The nozzle design starts by calculating the throat cross-section area. Eq. (1) can be used to calculate the nozzle throat cross-section area.

$$A_t = \frac{w_t}{P_t}\sqrt{\frac{R * T_t}{\gamma * M}} \tag{1}$$

To use this equation, the nozzle throat temperature and nozzle throat pressure must be calculated. Eq. (2) and Eq. (3) can be used to calculate the nozzle throat temperature and nozzle throat pressure.

$$T_t = \frac{T_c}{\left(1+\frac{\gamma-1}{2}\right)} \tag{2}$$

$$P_t = P_c\left(1+\frac{\gamma-1}{2}\right)^{\left(-\frac{\gamma}{\gamma-1}\right)} \tag{3}$$

From Eq. (2) and the given values in Table 2, the throat temperature can be calculated as 2667 Kelvin and from Eq. (3); the throat pressure can be calculated as 1.110 MPa.

Using the throat temperature as 2667 Kelvin, the throat pressure as 1.110 MPa, the universal gas constant and the molecular weight of 24 g/mol, the nozzle throat cross-section area can be calculated as 7.16cm^2.

Since the diameter is a function of the circular cross-sectional area, the diameter can be found. The nozzle throat diameter is calculated as 30.2 mm.

Using the throat diameter, the nozzle exit area can be calculated by also calculating the nozzle exit velocity. The velocity of the gas is measured relatively to the local speed of sound and is mentioned as the Mach number. The exit Mach number, M_e, can be found by using Eq. (4).

$${M_e}^2 = \left(\frac{2}{\gamma-1}\right)\left[\left(\frac{P_c}{P_a}\right)^{\left(\frac{\gamma-1}{\gamma}\right)} - 1\right] \tag{4}$$

The gas velocity increases while expanding in the divergent section of the nozzle therefore the pressure decreases. Ideally, when the gas exits the nozzle the gas flows full, which means the exit pressure is equal to the ambient pressure. Standard sea level conditions will be used in this thesis, so the standard ambient pressure is 101325 Pa (1 atm). Also, in the thesis the conditions will be based ideally, therefore the nozzle exit pressure is also 101325 Pa.

Using Eq. (4), the nozzle exit Mach number is calculated as 2.55 Mach.

To calculate the nozzle exit area Eq. (5) can be used.

$$A_e = \left(\frac{A_t}{M_e}\right)\left[\frac{1+\left(\frac{\gamma-1}{2}\right)M_e^2}{\frac{\gamma+1}{2}}\right]^{\left(\frac{\gamma+1}{2*\gamma-2}\right)} \tag{5}$$

With Eq. (5) the nozzle exit cross-section area is calculated as 24.18cm^2.

So, the nozzle exit diameter is found to be 55.49 mm. The expansion ratio, ε, is defined as the nozzle exit area divided by the nozzle throat area, which is calculated as 3.38.

A conical-shaped nozzle with a convergent angle of 45 degrees and a divergent angle of 15 degrees will be used since its recommended by Peters [Peters, 1965], as these values has almost become a standard because it is a good compromise of weight, length and performance. In addition, the radius of the wall contour at the throat section is ranging from 0.25 to 0.75 times the throat diameter.

The distance between the throat and exit plane is automatically determined as 49.18 mm by inputting the values obtained in this section.

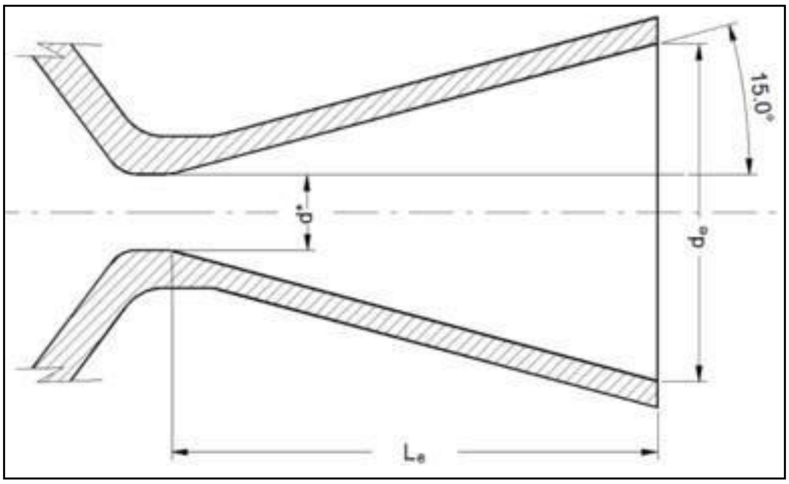

Figure 2: Geometry of conical-shaped nozzle [Peters, 1965].

To provide additional information, a correction factor called Thrust Efficiency is applied in the calculation of the exit gas momentum because of the performance losses that occur in a conical nozzle caused by non-axial components of the exhaust flow velocity. This factor can be expressed as below.

$$\lambda = \frac{1 + cos\alpha}{2} \tag{6}$$

For α being equal to 15 degrees, the correction factor, λ, will be 0.983 [Peters, 1965].

DESIGN OF BELL-SHAPED NOZZLE

The bell-shaped nozzle was developed with the purpose of obtaining a much lighter nozzle while gaining higher performance. With the fast expansion in the diverging section, the flow velocity increases much faster while the diverging section is changing enough to still prevent oblique shocks. An equivalent 15-degree half angle conical nozzle like the one designed for the conical-shaped nozzle is usually used as a standard to specify bell nozzles. In this thesis, an 80% bell nozzle is compared to a 15-degree half angle conical nozzle. The length between the throat and exit section of the 80% bell nozzle is 80% of that of the 15-degree half angle conical-shaped nozzle, while still having the same throat area, below the throat radius and expansion ratio [Rao, 1958].

Operating Conditions

The operating conditions mentioned above are also used for the bell-shaped nozzle, to provide a fair comparison between the nozzles.

Bell-shaped Nozzle Design Calculations

A suited way to design an optimum bell-shaped contour is by using the parabolic approximation proposed by Rao. The configuration of this design is shown in Fig. 3 [Rao, 1958].

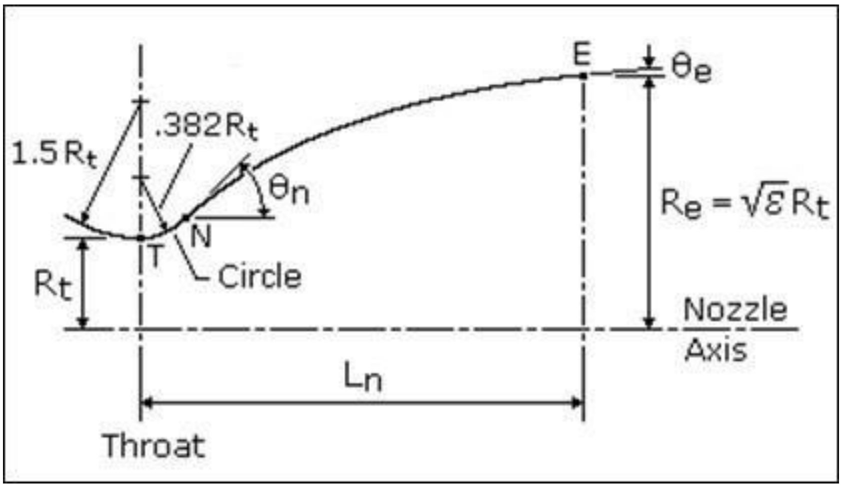

Figure 3: Design configuration of a parabolic approximation bell nozzle [Rao, 1958]

The design of a nozzle by this approximation requires the throat diameter, D_t, the distance between the throat and exit plane L_n, the expansion ratio ε, the initial contour angle of the beginning of the parabola Θ_n, and the contour exit angle of the parabola Θ_e.

From the conical nozzle design calculations, the throat diameter was calculated as 30.2 mm, the expansion ratio was calculated as 3.38. The distance between the throat and the exit plane will be 80% of the length of the conical nozzle designed, which is equal to 39.35 mm.

For the beginning and exit angles of the parabola, Fig. 4 can be used from Ref. [3].

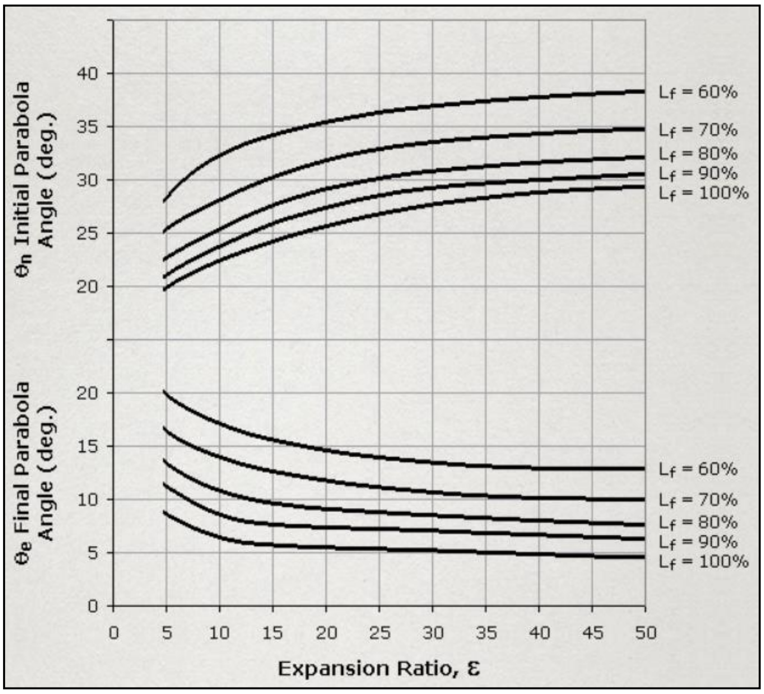

Figure 4: Initial and final parabola angle as function of expansion ratio [3]

From Fig. 4, Θ_n and Θ_e can be obtained as 23.6 and 15 degrees for the fractional length of 80% and an expansion ratio of 3.38. For not so high operating conditions the values obtained so far is enough to approximately design the nozzle with the parabolic approximation method of Rao.

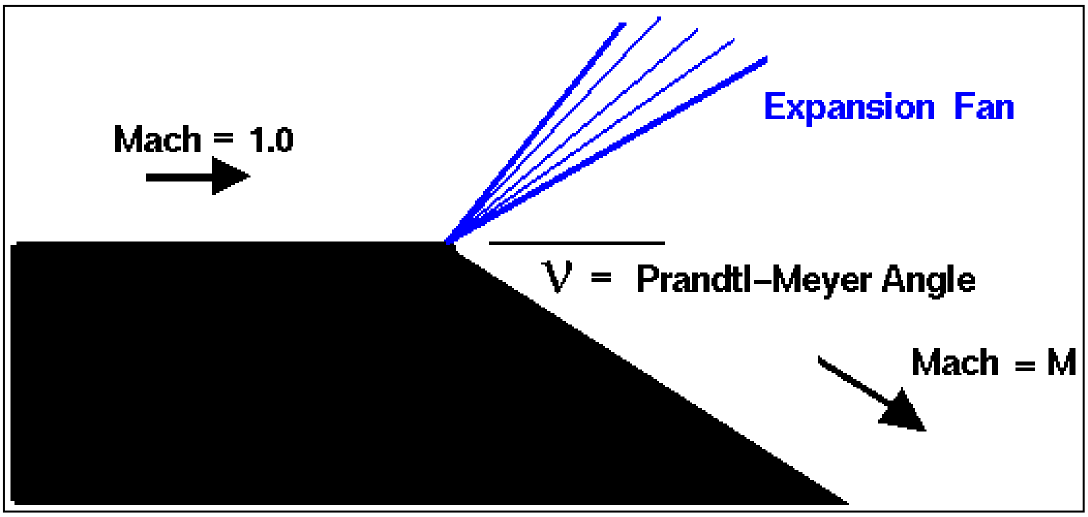

Figure 5: Illustrated location of the Prandtl-Meyer Angle [7]

Also as illustrated in Fig. 5, the Mach number of a sonic/supersonic flow increases with an expansion fan. The greater the incoming Mach number or angle the more increase in the exit Mach number. For a supersonic nozzle, the Mach number in the nozzle throat is mostly fixed to one, so only the change in the angle is of interest. This angle is called the Prandtl-Meyer Angle, v.

To find this angle, the Prandtl Meyer function in Equation (7) can be used.

$$\nu = \sqrt{\frac{\gamma+1}{\gamma-1}}\, tan^{-1}\left(\sqrt{\frac{\gamma-1}{\gamma+1}(M_e{}^2-1)}\right) - tan^{-1}\sqrt{(M_e{}^2-1)} \tag{7}$$

The meaning of the Prandtl-Meyer function is that it is the angle at which a sonic flow must expand to obtain a given Mach number.

With Equation (7), the Prandtl-Meyer Angle can be found as 47.16 degrees for 2.55 Mach. Θ_n can be found as the half of the Prandtl-Meyer Angle, which is 23.58 degrees [7].

For additional information, a more precise design can be done with the method of characteristics. The details of this method are not investigated in this thesis, therefore a MATLAB code of Olson [8] is used to directly give the contour of the divergent section of the bell nozzle. This is only used to crosscheck the design calculations made before.

RESULTS AND DISCUSSION

Analysis of Conical-shaped Nozzle

2-D CFD Analysis of Conical-shaped Nozzle

Fig. 6 shows the static pressure in the conical-shaped nozzle. It has a maximum value of 1.9 MPa and a minimum value of 0.1 MPa. The pressure exactly at the throat section varies from 0.8 MPa to 1.2 MPa, the theoretical value of the throat pressure was found to be 1.1 MPa. The different pressure areas can be seen in the diverging section of the nozzle.

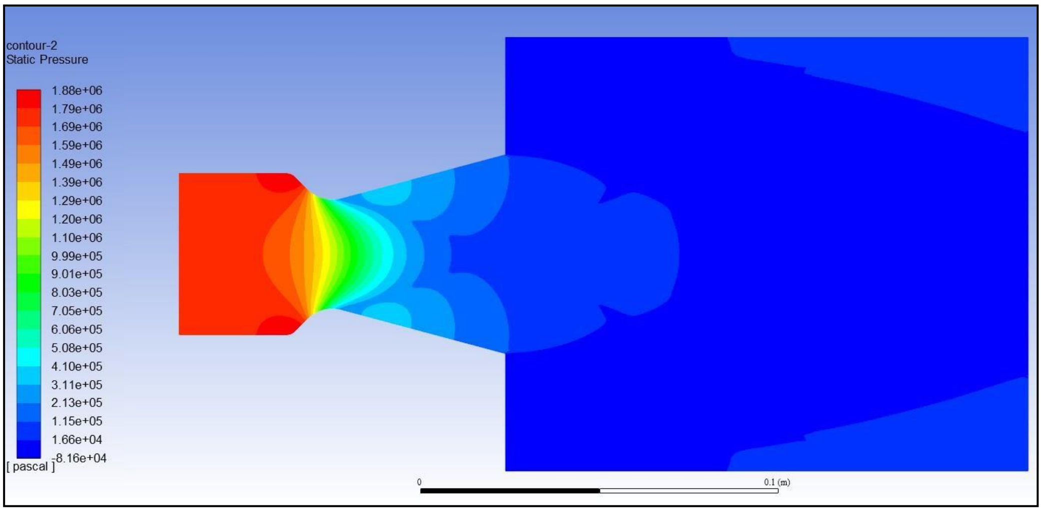

Figure 6: 2-D CFD analysis of conical-shaped nozzle with static pressure presentation

In Fig. 7, presentation of the Mach number can be seen. A maximum Mach number of 3.9 Mach is obtained and the Mach number at the throat is equal to 1.0, confirming the theoretical findings but the Mach number at the nozzle exit section varies from 1.8 Mach to 2.55 Mach. Theoretically it must be 2.55 Mach but only a little section of the main flow core can be seen as 2.55 Mach. This is related to the different pressure areas shown in Fig. 6. A weak shock occurs right after the throat section, which can be seen in Fig. 7 [5]. Because of this, the total pressure increases instantly and the Mach number decreases upstream the shock wave. The core of the flow is not so much effected as the divergent contour; therefore, at the nozzle exit area the Mach number is still able to obtain the theoretical value of 2.55 Mach.

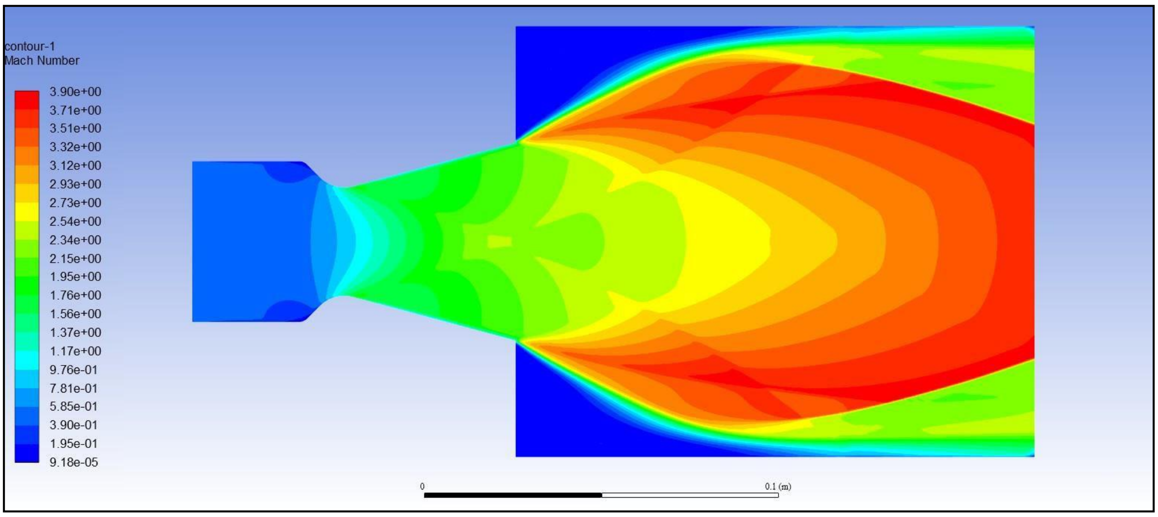

Figure 7: 2-D CFD analysis of conical-shaped nozzle with Mach number presentation

In Fig. 8, the temperature distribution due to these effects inside the nozzle can be seen with a maximum temperature of 3000 Kelvin and a minimum temperature of 600 Kelvin.

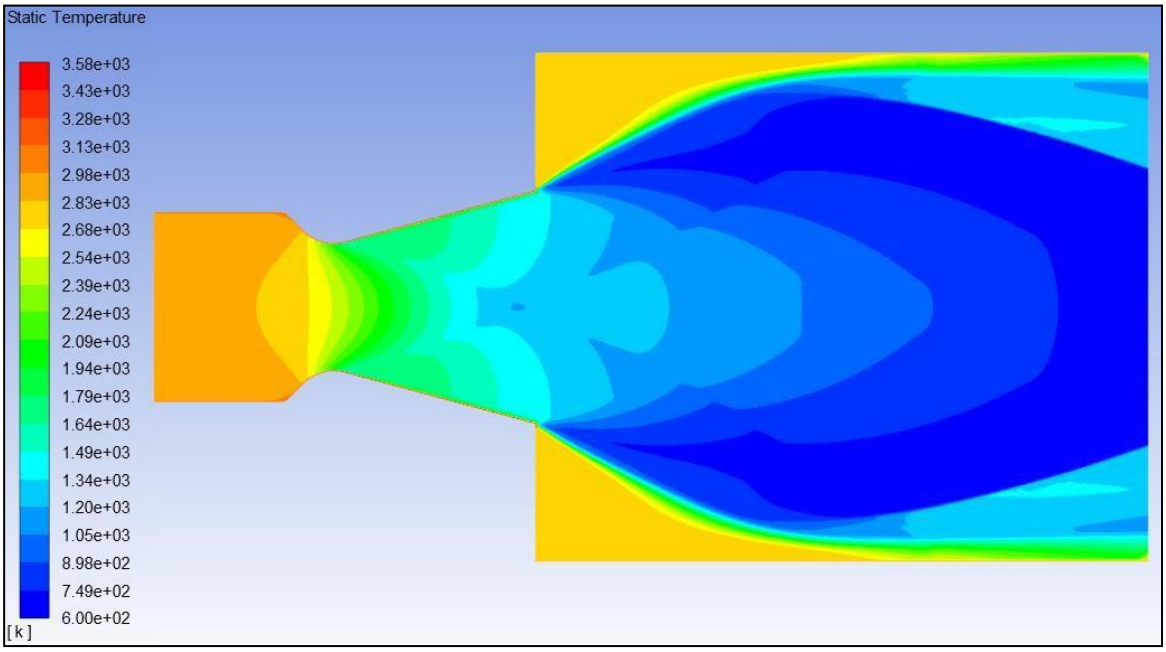

Figure 8: 2-D CFD analysis of conical-shaped nozzle with temperature presentation

3-D Static Structural Analysis of Conical Nozzle

Analysis for Molybdenum

Fig. 9 shows the total deformation due to the pressure and temperature effects of the molybdenum conical nozzle with a maximum total deformation of $5.1453e^{-3}$ mm.

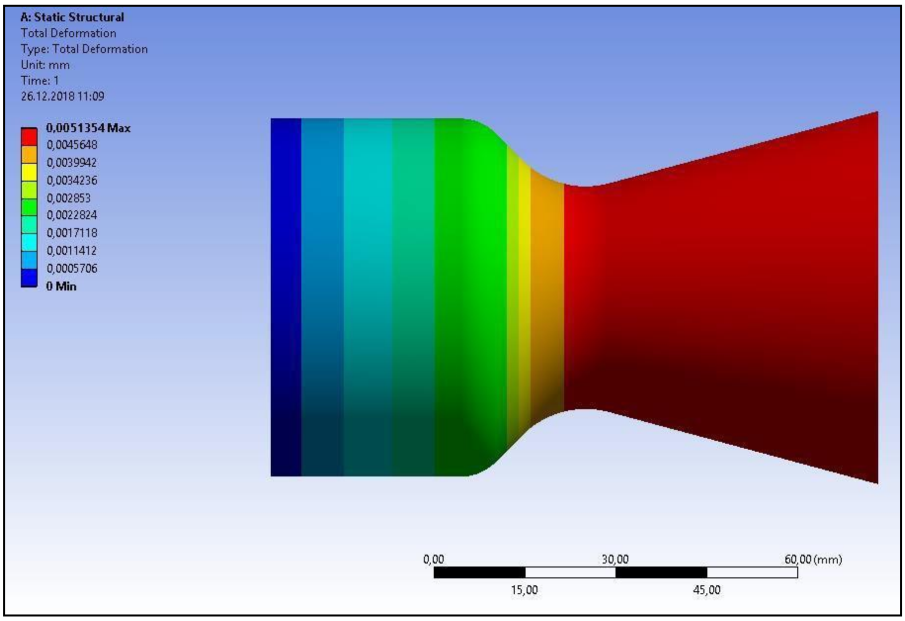

Figure 9: 3-D static structural analysis of conical-shaped nozzle with total deformation presentation for molybdenum

Fig. 10 shows the normal elastic strain in the x-axis to be a maximum of $\mathbf{1.5345}\boldsymbol{e^{-4}}$ mm/mm, which is positive which means tension, and a minimum of $-\mathbf{2.409}\boldsymbol{e^{-5}}$ mm/mm, which is negative which means compression.

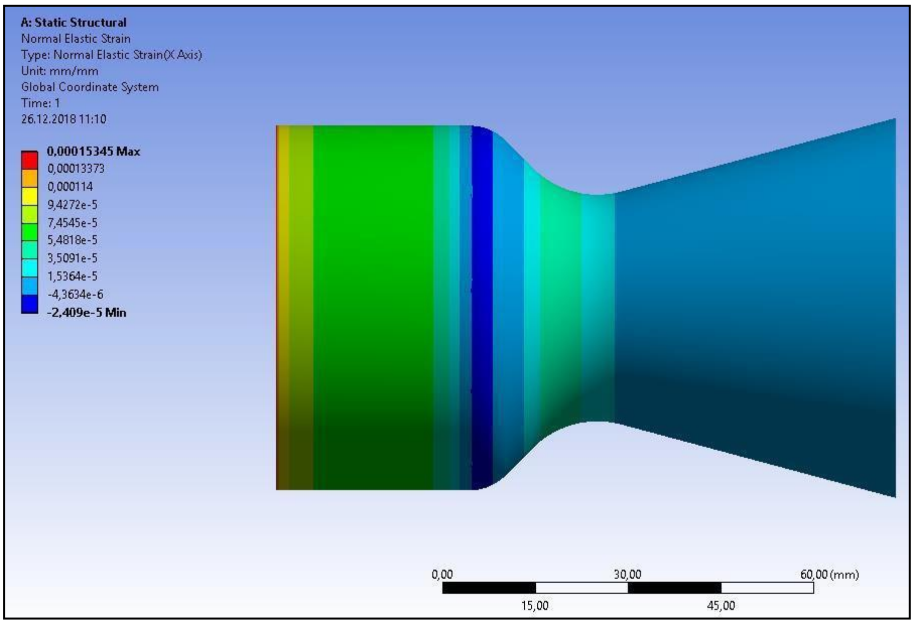

Figure 10: 3-D static structural analysis of conical-shaped nozzle with elastic strain presentation for molybdenum

Fig. 11 is showing the temperature distribution for the molybdenum conical nozzle. The outer shell has reached a temperature between 700-1000 Kelvin.

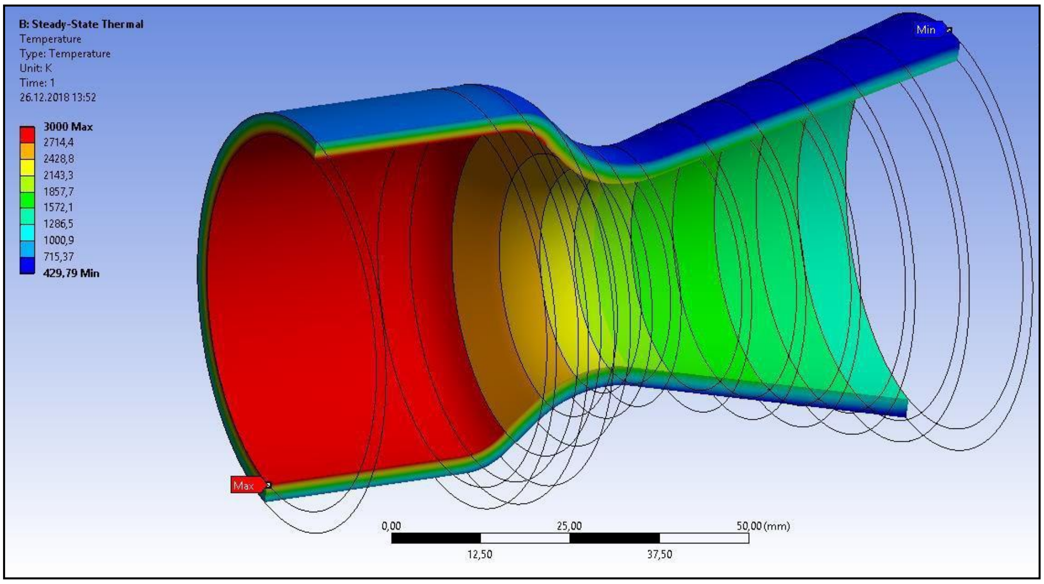

Figure 11: 3-D static structural analysis of conical-shaped nozzle with temperature distribution presentation for molybdenum

Analysis for Titanium

Fig. 12 shows the total deformation due to the pressure and temperature effects of the titanium conical nozzle with a maximum total deformation of $1.5138e^{-2}$ mm.

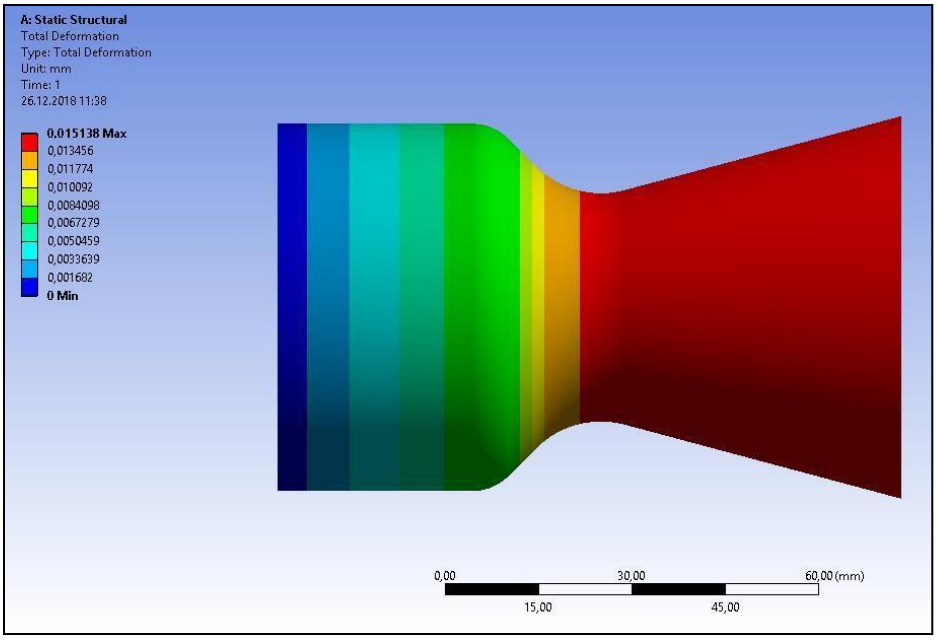

Figure 12: 3-D static structural analysis of conical-shaped nozzle with total deformation presentation for titanium

Fig. 13 shows the normal elastic strain in the x-axis to be a maximum of $\mathbf{4.3599}e^{-4}$mm/mm, which is positive which means tension, and a minimum of $-\mathbf{7.486}e^{-5}$mm/mm, which is negative which means compression.

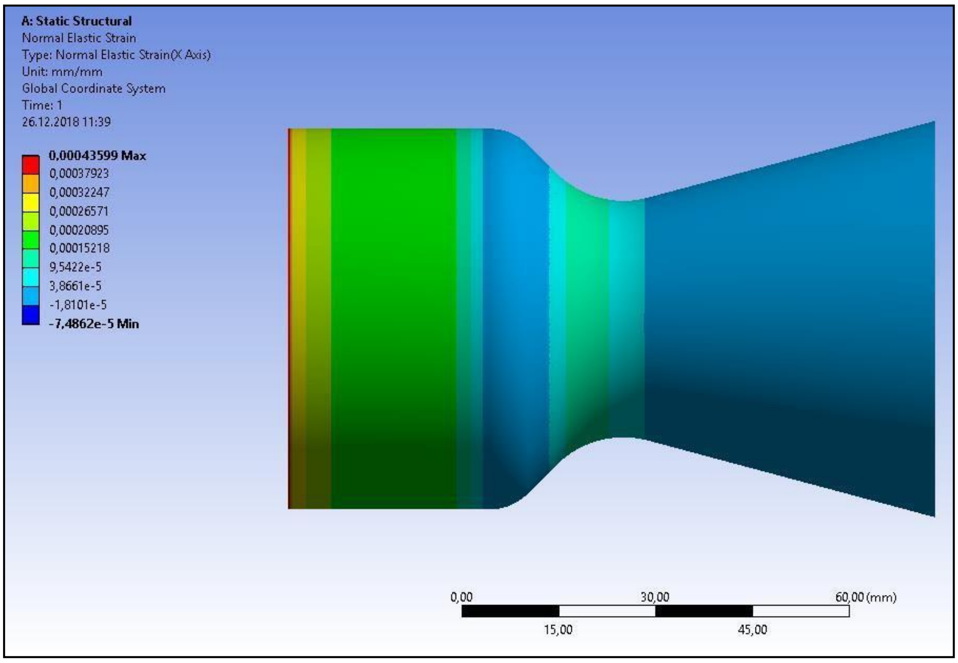

Figure 13: 3-D static structural analysis of conical-shaped nozzle with elastic strain presentation for titanium

Fig. 14 is showing the temperature distribution for the titanium conical nozzle. The outer shell has reached a temperature between 2300-2600 Kelvin.

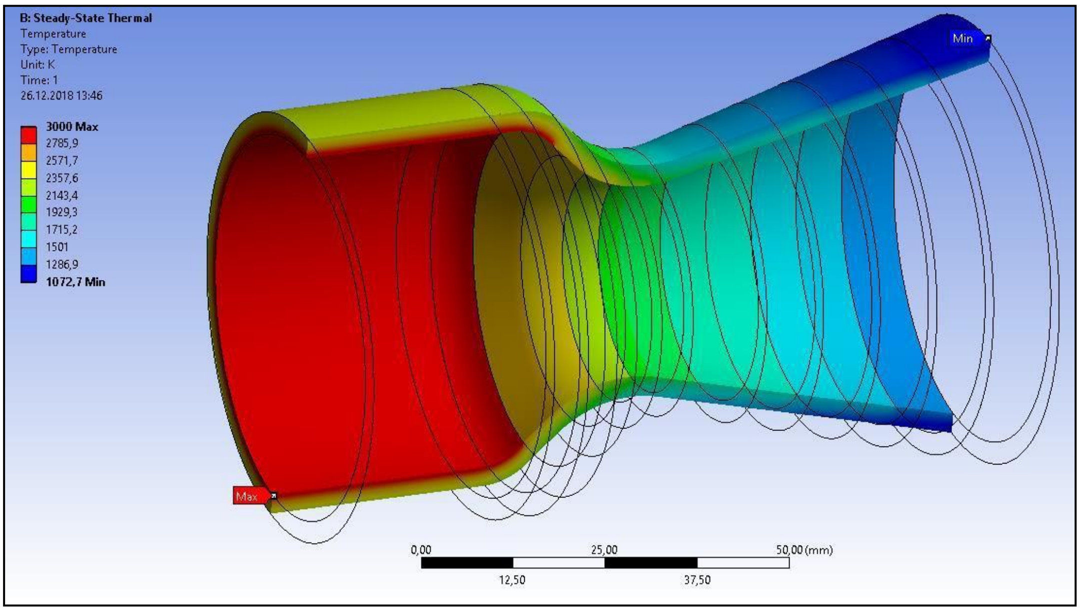

Figure 14: 3-D static structural analysis of conical-shaped nozzle with temperature distribution presentation for titanium

Analysis of Bell-shaped Nozzle

2-D CFD Analysis of Bell-shaped Nozzle

Fig. 15 shows the static pressure in the bell-shaped nozzle. It has a maximum value of 1.9 MPa and a minimum value of 0.15 MPa. The pressure exactly at the throat section varies from 0.8 MPa to 1.2 MPa, the theoretical value of the throat pressure was found to be 1.1 MPa. The different pressure behavior can be seen in the diverging section of the nozzle.

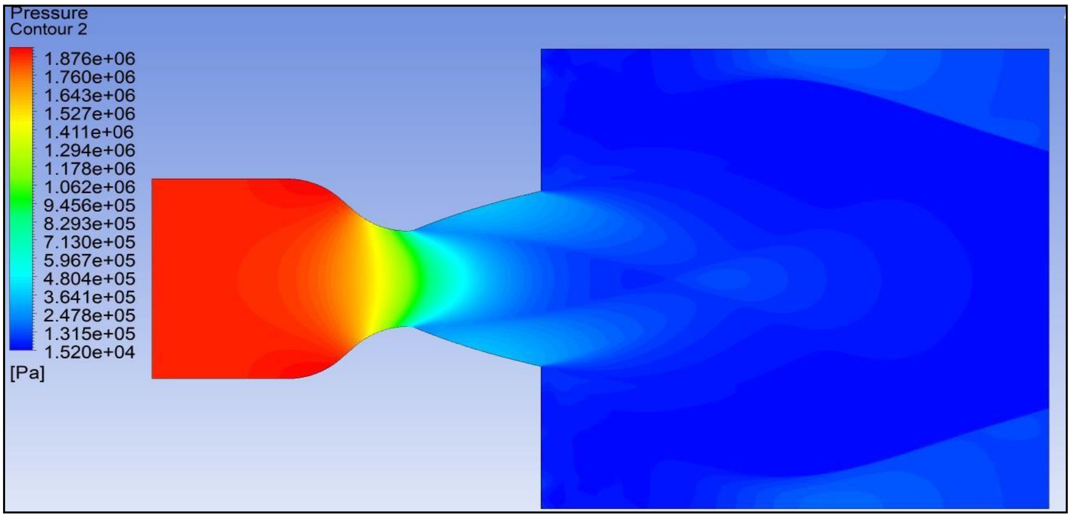

Figure 15: 2-D CFD analysis of bell-shaped nozzle with static pressure presentation

In Fig. 16, presentation of the Mach number can be seen. A maximum Mach number of 4.0 Mach is obtained and the Mach number at the throat is equal to 1.0, confirming the theoretical findings but the Mach number at the nozzle exit section varies from 2.0 Mach to 2.6 Mach. Theoretically is must be 2.55 Mach but this is a little (but larger than the conical nozzle) section of the main flow core can be seen around 2.55 Mach. This is again, related to the different pressure behavior shown in Fig. 15.

Again, a weak shock occurs right after the throat section, which can be seen in Fig. 16, but this time the effect on the main flow core is not so much as in the conical nozzle because of the shape of the bell, which has a gradually decreasing slope. Therefore, a much larger section of the main core flow can be seen unaffected and to be around 2.55 Mach, which allows for obtaining a higher maximum Mach number in the plume [Sutton, 2006].

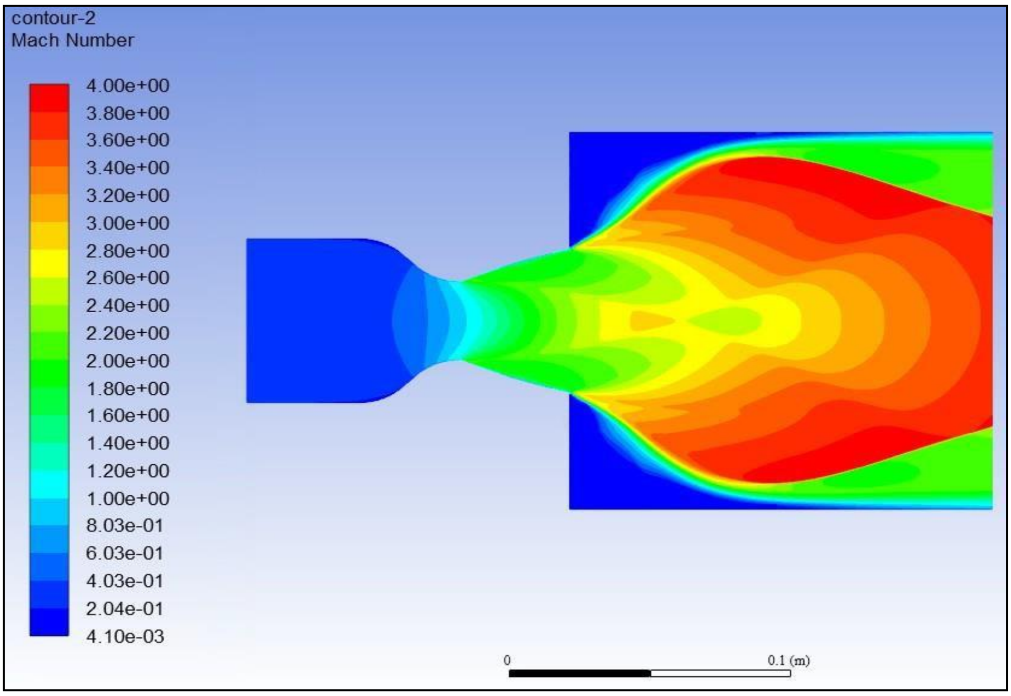

Figure 16: 2-D CFD analysis of bell-shaped nozzle with Mach number presentation

In Fig. 17, the temperature distribution due to these effects inside the nozzle can be seen with a maximum temperature of 3000 Kelvin and a minimum temperature of 575 Kelvin, which is slightly lower than the conical nozzle.

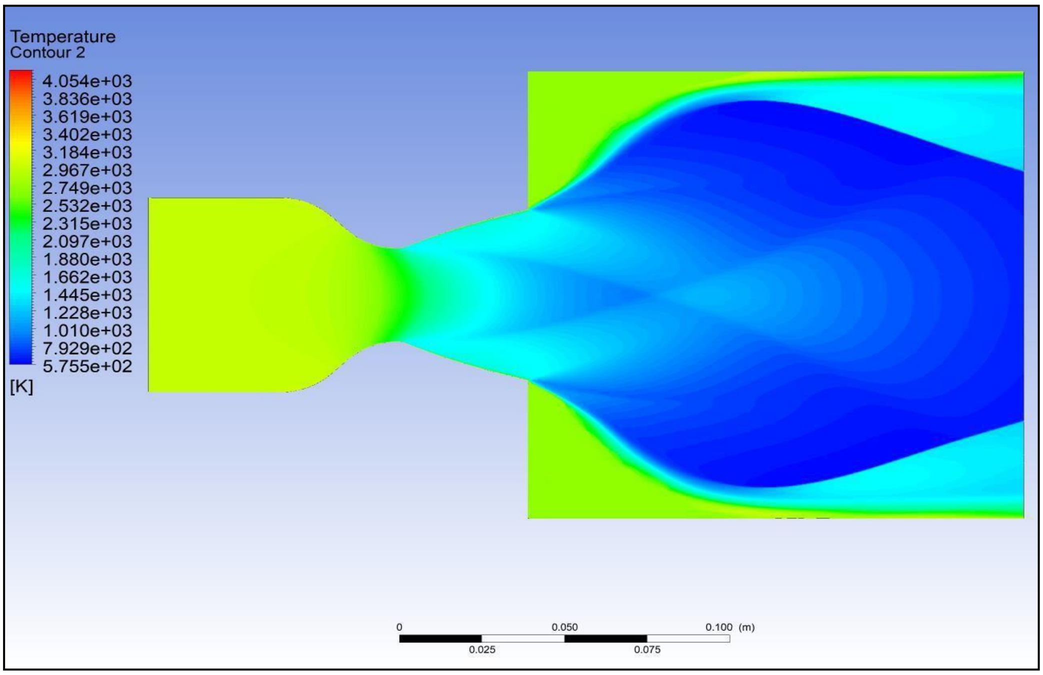

Figure 17: 2-D CFD analysis of bell-shaped nozzle with temperature presentation

3-D Static Structural Analysis of Bell Nozzle

Analysis for Molybdenum

Fig. 18 shows the total deformation due to the pressure and temperature effects of the molybdenum bell nozzle with a maximum total deformation of 5.017e^{-3}mm.

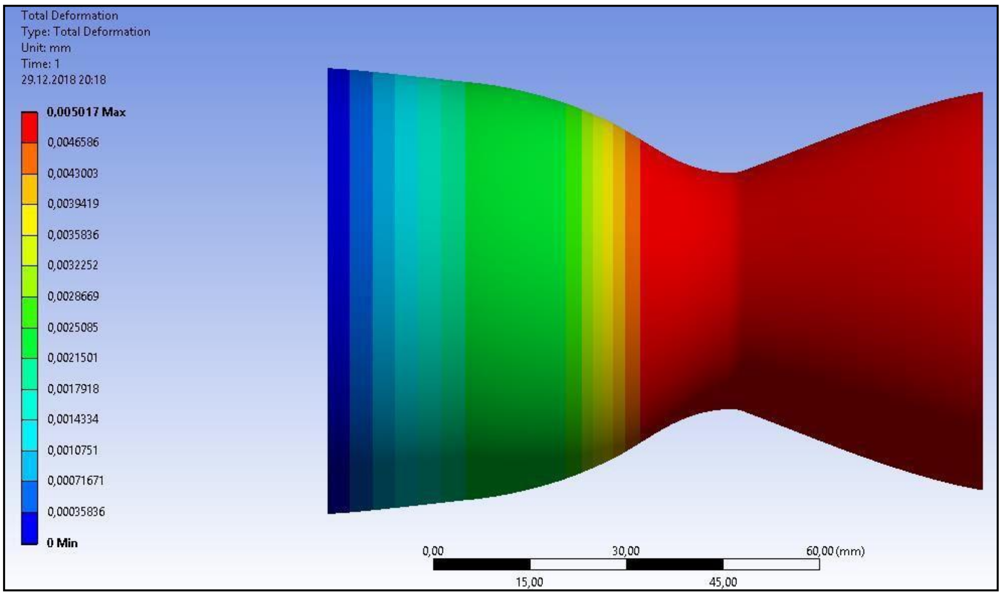

Figure 18: 3-D static structural analysis of bell-shaped nozzle with total deformation presentation for molybdenum

Fig. 19 shows the normal elastic strain in the x-axis to be a maximum of $\mathbf{1.4682}e^{-4}$mm/mm, which is positive, which means tension, and a minimum of $\mathbf{9.67}e^{-8}$mm/mm.

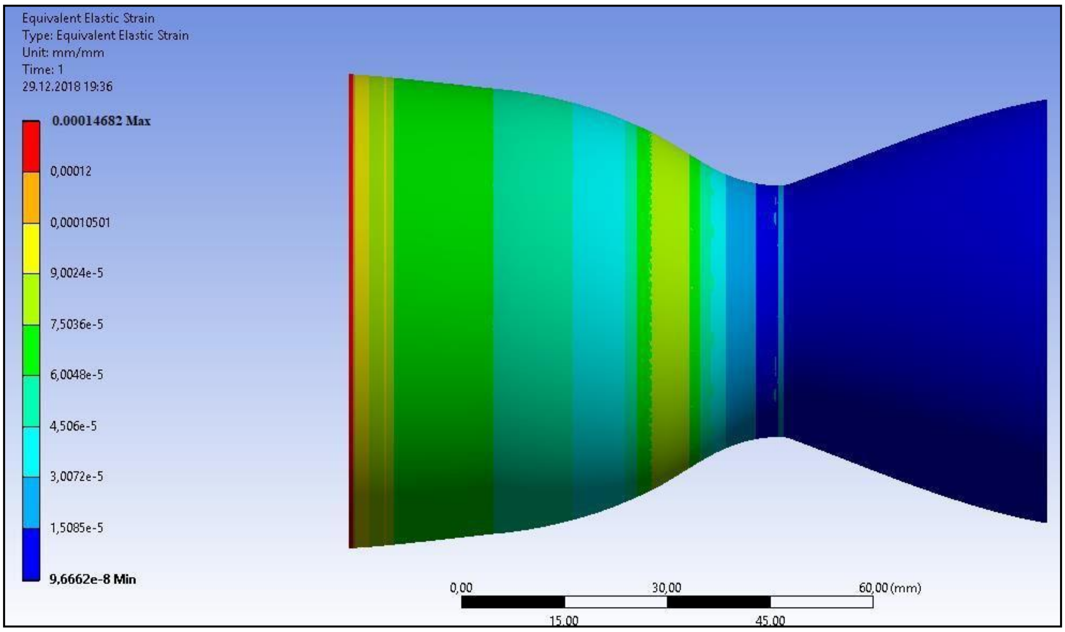

Figure 19: 3-D static structural analysis of bell-shaped nozzle with elastic strain presentation for molybdenum

Fig. 20 is showing the temperature distribution for the molybdenum conical nozzle. The outer shell has reached a temperature between 400-800 Kelvin.

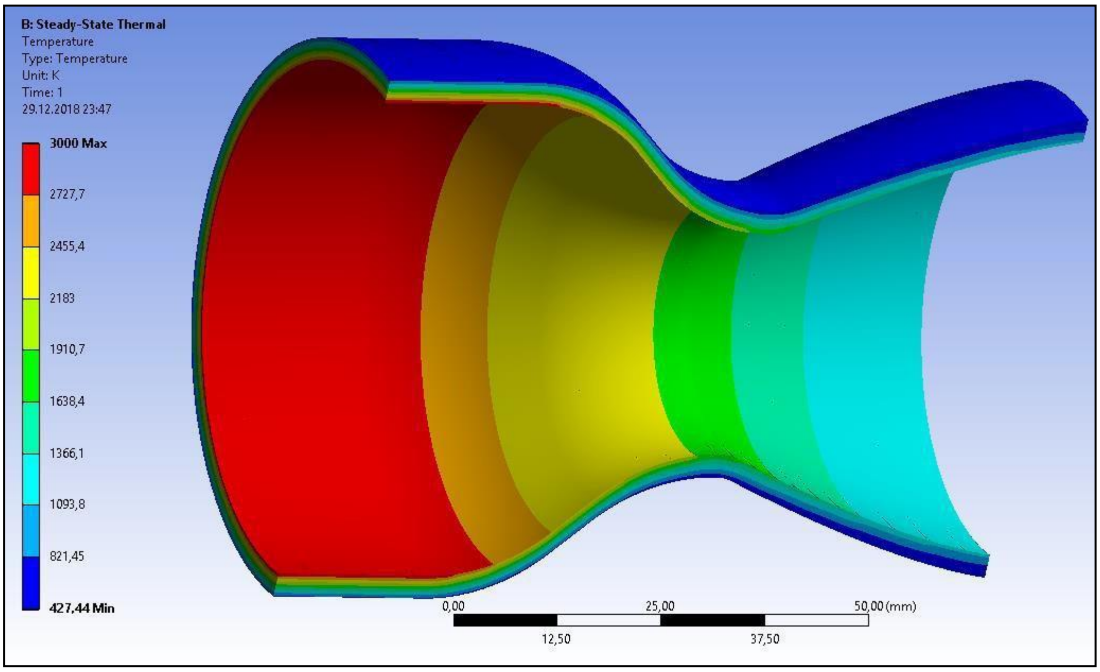

Figure 20: 3-D static structural analysis of bell-shaped nozzle with temperature distribution presentation for molybdenum

Analysis for Titanium

Fig. 21 shows the total deformation due to the pressure and temperature effects of the titanium conical nozzle with a maximum total deformation of $1.4879e^{-2}$ mm.

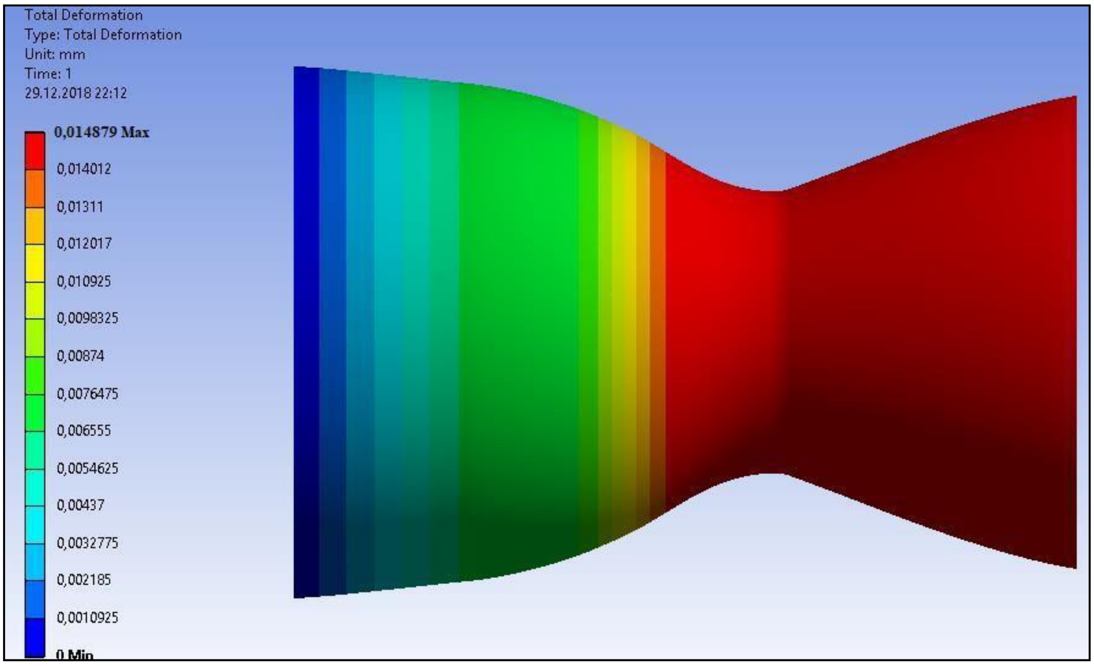

Figure 21: 3-D static structural analysis of bell-shaped nozzle with total deformation presentation for titanium

Fig. 22 shows the normal elastic strain in the x-axis to be a maximum of $\mathbf{4.2295}\boldsymbol{e}^{-4}$mm/mm, which is positive, which means tension, and a minimum of $\mathbf{1.064}\boldsymbol{e}^{-6}$ mm/mm.

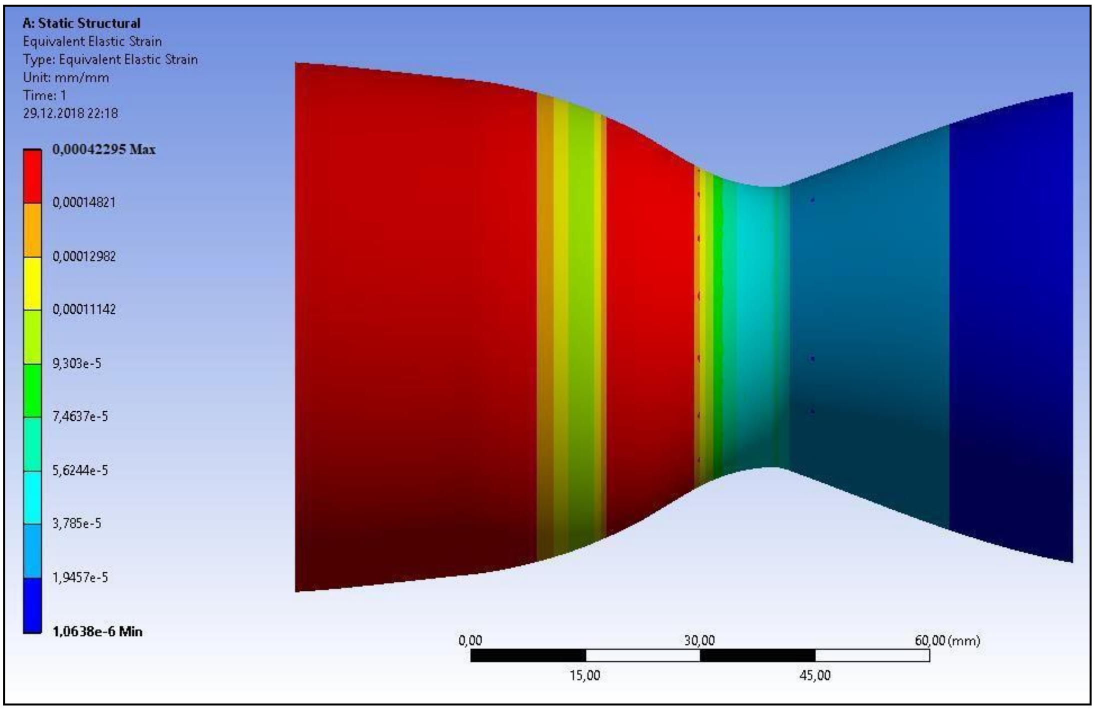

Figure 22: 3-D static structural analysis of bell-shaped nozzle with elastic strain presentation for titanium

Fig. 23 is showing the temperature distribution for the titanium conical nozzle. The outer shell has reached a temperature between 2100-2350 Kelvin.

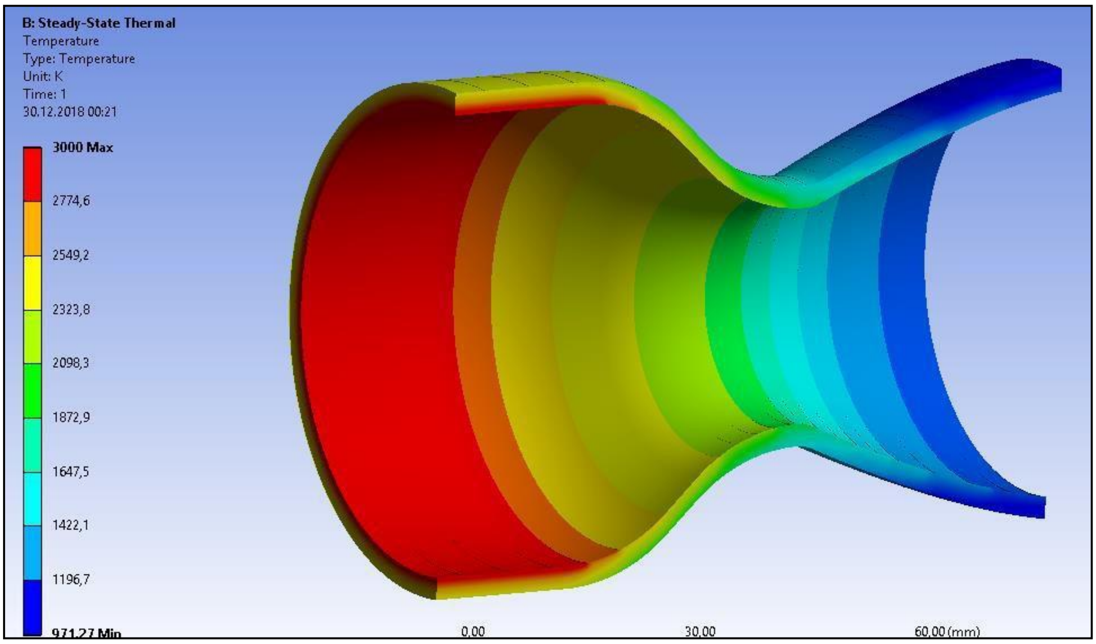

Figure 23: 3-D static structural analysis of bell-shaped nozzle with temperature distribution presentation for titanium

Results Overview

All the results obtained in the section above can be seen in Table 3 for a quick view.

Table 3: Results Overview

Nozzle Type	Matching Exit Mach Number Section Percentage (%)	Total Deformation (mm)	Min. Elastic Strain (mm/mm)	Max. Elastic Strain (mm/mm)	Outer Shell Temp. (K)
Molybdenum Conical Nozzle	8	$5.1453e^{-3}$	$-2.409e^{-5}$	$1.5345e^{-4}$	400-1000
Titanium Conical Nozzle	8	$1.5138e^{-2}$	$-7.486e^{-5}$	$4.3599e^{-4}$	2300-2600
Molybdenum Bell Nozzle	37	$5.017e^{-3}$	$9.67e^{-8}$	$1.4682e^{-4}$	400-820
Titanium Bell Nozzle	37	$1.4879e^{-2}$	$1.064e^{-6}$	$4.2295e^{-4}$	2100-2350

CONCLUSION

Comparing the static pressure and Mach number presentations of the conical nozzle and bell nozzle, it can be said that the bell nozzle reduces the negative effects by reducing the effects of the weak shock waves occurring in the nozzle divergent section on the core flow with its gradually decreasing divergent contour.

Thereby it obtains a slightly better performance by reaching a higher maximum Mach number of 4.0 while operating at the same conditions with the conical nozzle, which reaches a maximum Mach number of 3.90.

Also, by obtaining a higher average Mach number inside the nozzle, the pressure inside the nozzle is decreased and thereby decreasing the structural effects on the nozzle walls. This can be seen by comparing the 3-D total deformation and elastic strain presentations for Titanium and Molybdenum for both of the nozzles. It can clearly be seen that the total deformation and elastic strain slightly decreases for the bell nozzle because of these reasons.

In addition, there is a slightly decrease in the temperature at the nozzle walls for the bell nozzle as can be seen for Molybdenum when comparing the temperature distribution presentations. The outer face of the nozzle reaches a maximum between 400 and 1000 Kelvin for the conical nozzle while between 400 and 820 Kelvin for bell nozzle. The same kind of observation can be seen for Titanium.

This concludes that the bell nozzle outperforms the conical nozzle for the design conditions given, while being shorter thus lighter than the conical nozzle.

There could be a possibility where a molybdenum conical nozzle, which just scarcely could not operate at a certain condition, could be replaced by a molybdenum bell nozzle with the slightly improved structural numbers, which could operate.

Keeping in mind that the manufacturability and the manufactory costs of the bell nozzle could be higher than the conical nozzle because of its complex design.

Also, both Molybdenum and Titanium can’t withstand the inside temperatures practically. With a melting point around 2600 Celsius degrees for Molybdenum and 1700 Celsius degrees for Titanium, it will melt if there is no cooling system. Here, only the system without a cooling system has been investigated.

REFERENCES

[1] Besnard, E., and Garvey, J., Development and Flight-Testing of Liquid Propellant Aerospike Engines, 40th AIAA/ASME/SAE/ASEE Joint Propulsion Conference and Exhibit, AIAA Paper 2004-3354, Fort Lauderdale, FL, 14 July 2004.

[2] Chapman, D., Huehn, D., and Larson, H., Investigation of Separated Flows in Supersonic and Subsonic Streams with Emphasis on the Effect of Transition, NACA Rept. 1536, Ames Aeronautical Lab., Moffet Field, CA, 1958.

[3] Https://www.braeunig.us/space/propuls.htm (Nov, 2018)

[4] Http://www.engr.uconn.edu/~barbertj/CFD%20Training/Fluent/4%20Solver%20Settings.pdf (Dec, 2018)

[5] Https://www.grc.nasa.gov/www/k-12/airplane/crosshock.html (Dec, 2018)

[6] Https://www.grc.nasa.gov/www/k-12/airplane/mach.html (Dec, 2018)

[7] Https://www.grc.nasa.gov/www/k-12/airplane/pranmyer.html(Nov, 2018)

[8] Https://www.mathworks.com/matlabcentral/fileexchange/14682-2-d-nozzle-design (Nov,2018)

[9] Https://www.risacher.org/rocket/ (Nov, 2018)

[10] Keenan, Chao, Kaye, (1983) *Gas Tables*, Wiley, New York.

[11] Östlund, J., and Bigert, M., A Subscale Investigation on Side Loads in Sea Level Rocket Nozzle, 35th AIAA/ASME/SAE/ASEE Joint Propulsion Conference and Exhibit, AIAA Paper 1999-2759, Fort Lauderdale, FL, 20–24 July 1999.

[12] Peters R. L., (1965) Design of Liquid, Solid, and Hybrid Rockets, Hayden Book Co. Inc., New York.

[13] Rao G. V. R., Contoured Rocket Nozzles, Ninth annual congress of the International Astronautical Federation 1958, Library of Congress.

[14] Stark, R., Flow Separation in Rocket Nozzles, a Simple Criteria, 41st AIAA/ASME/SAE/SEE Joint Propulsion Conference, AIAA Paper 2005-3940, Tucson, AZ, 13 July 2005.

[15] Stark, R., and Nürnberger-Génin, C., Experimental Study of Dual Bell Nozzle, Second European Conference for Aerospace Science (EUCASS), Bruxelles, Belgium, July 2007.

[16] Sutton G. P., Biblarz O., (2000) Rocket Propulsion Elements: an Introduction to the Engineering of Rockets, 7th Ed., John Wiley &Sons Ltd, New York.

[17] Sutton G. P., (2006) History of Liquid Propellant Rocket Engines, AIAA.